

Fig. S1. XRD spectra of  $\text{MAPbI}_{3-x}\text{Cl}_x$  films exposed to  $\text{O}_3$  (dark orange) and TMA/ $\text{O}_3$  (orange).

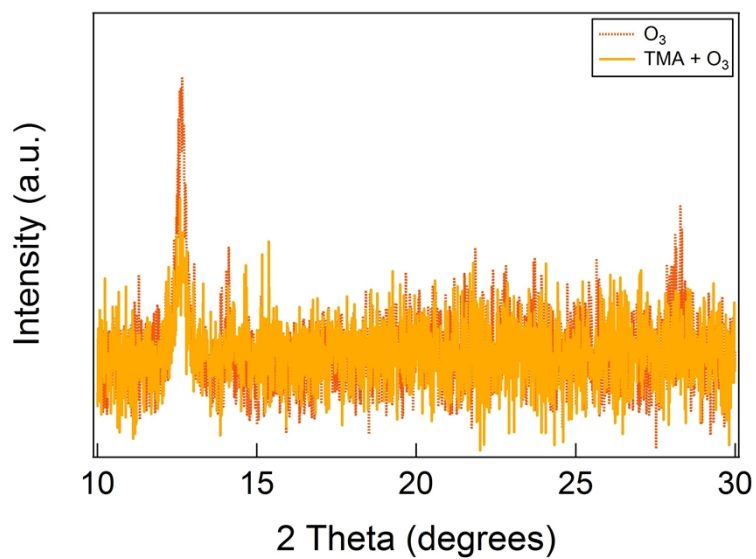
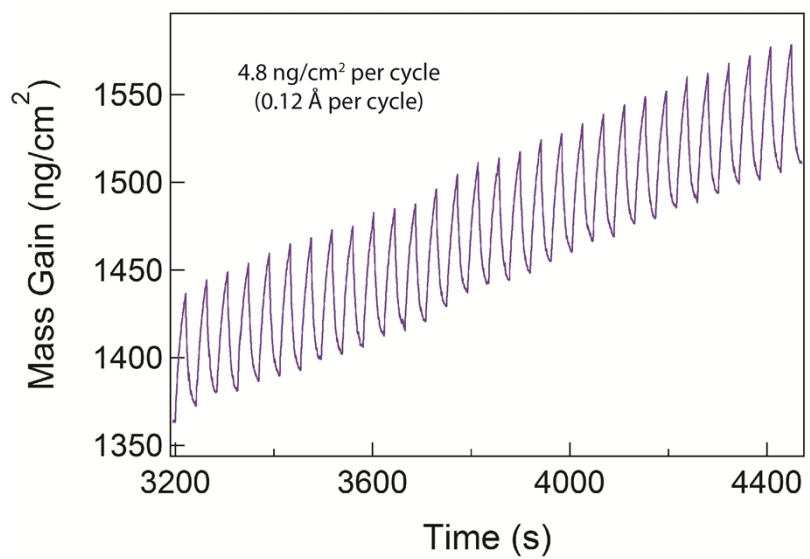


Fig. S2. In-situ quartz crystal microbalance (QCM) data recorded during 30 cycles of *nh*-Al<sub>2</sub>O<sub>3</sub> ALD.



Video S3. Degradation of  $\text{MAPb}_{3-x}\text{Cl}_x$  films upon contact with 5  $\mu\text{L}$  water droplet. Unpassivated, 3 nm *nh*- $\text{Al}_2\text{O}_3$ , and 18 nm *hb*- $\text{Al}_2\text{O}_3$  (left to right).

VIDEO S3

Fig. S4. Degradation of  $\text{MAPbI}_{3-x}\text{Cl}_x$  films in RH 85% as a function of time. Unpassivated, 3 nm *nh*- $\text{Al}_2\text{O}_3$ , and 18 nm *hb*- $\text{Al}_2\text{O}_3$  (left to right). a), b), and c) correspond to  $t = 0, 6,$  and  $48$  h, respectively.

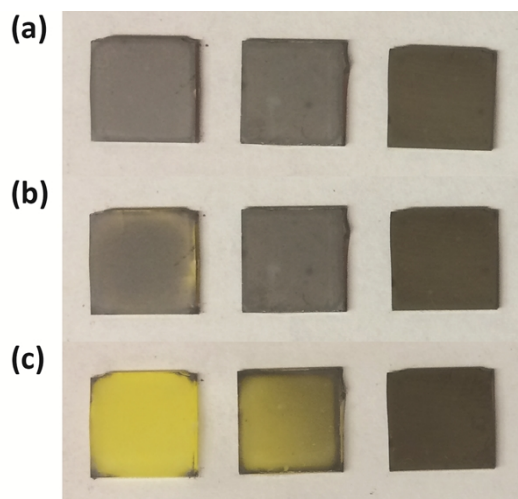
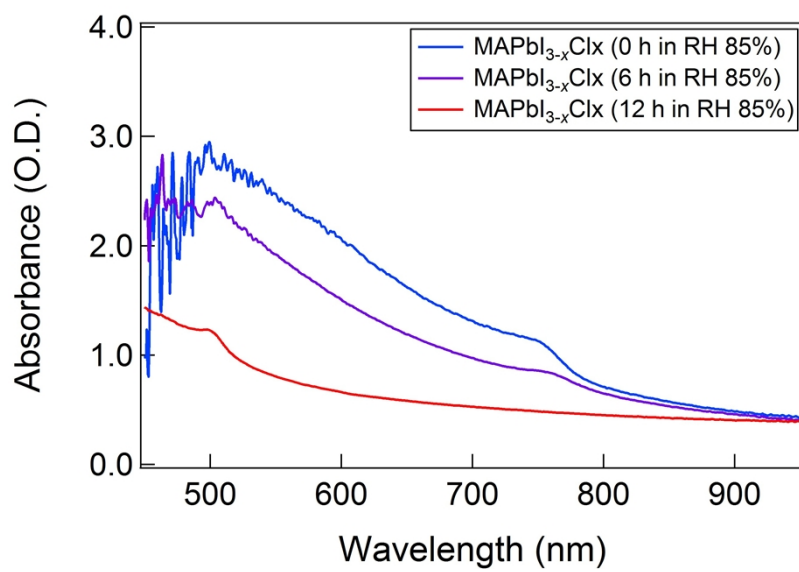


Fig. S5. UV-vis spectra of unpassivated MAPbI<sub>3-x</sub>Cl<sub>x</sub> films in RH 85% as a function of time.



Video S6. Degradation of MAPb<sub>3-x</sub>Cl<sub>x</sub> films upon heating on a hotplate at 250 °C in N<sub>2</sub> filled glove box.

VIDEO S6

Fig. S7. FTIR spectra of unpassivated and 18 nm *hb*-Al<sub>2</sub>O<sub>3</sub> passivated MAPbI<sub>3-x</sub>Cl<sub>x</sub> films before and after annealing at 250 °C in a N<sub>2</sub> filled glove box.

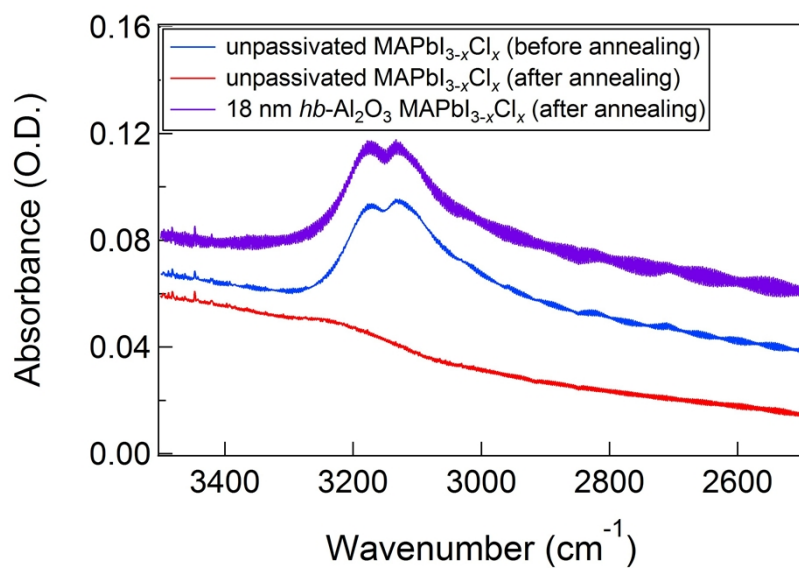


Fig. S8. XRD spectra of unpassivated, 3 nm *nh*-Al<sub>2</sub>O<sub>3</sub>, and 18 nm *hb*-Al<sub>2</sub>O<sub>3</sub> passivated MAPbI<sub>3-x</sub>Cl<sub>x</sub> films after annealing at 250 °C in N<sub>2</sub> filled glove box (t = 70 s).

